IHJPAS. 36 (4) 2023

Ibn Al-Haitham Journal for Pure and Applied Sciences
Journal homepage: jih.uobaghdad.edu.iq

Building an Analytical Method to Study Cantilever Beam Dynamic Response

Samaher Mohammed Sarhan
Department of Mechatronics Engineering, Al-Khwarizmi
College of Engineering, University of Baghdad,
Baghdad, Iraq.

Article history: Received 13 December 2022, Accepted 14 March 2023, Published in October 2023

doi.org/10.30526/36.4.3140

Abstract

Cantilever beams are used in many crucial applications in machinery and construction. For example, the airplane wing, the microscopic probe for atomic force measurement, the tower crane overhang and twin overhang folding bridge are typical examples of cantilever beams. The current research aims to develop an analytical solution for the free vibration problem of cantilever beams. The dynamic response of AISI 304 beam represented by the natural frequencies was determined under different working surrounding temperatures ((-100 ℃ to 400 ℃)). A Matlab code was developed to achieve the analytical solution results, considering the effect of some beam geometrical dimensions. The developed analytical solution has been verified successfully with real experimental data and the error was not exceeded 1%.

Keywords: analytical solution, cantilever beam, free vibration, mathematical modeling.

1. Introduction

The mathematical modeling of the vibration properties of the cantilever beam seems a crucial topic due to its wide range of applications in structural and construction technology and other sectors. In service conditions, those cantilever beams expose to various levels of vibrations that influence their functional behavior. The prolonged working under such vibration conditions

threatens the performance stability of those vital structural parts [1].

Studying the response of the cantilever beam to the applied vibration is an important issue because it enables us to analyze and interpret a variety of typical real cases, as stated in the examples above. These applications can be molded as cantilever beam that gives flexibility in design tuning for the most effective real systems. The vibration analysis is one of the most important and effective analyses of the structure in different industrial sectors. Where, the vibration results can be assisted to identify faults or detect warning signs of potential failures. It can also aid in the detection of misalignment or unbalance of assets such as bearings and rotating pieces of equipment.

A cantilever beam will oscillate at its natural frequency when given a stimulus and left to vibrate on its own. Free vibration is the name given to this state. The system's mass and stiffness parameters are the only ones that affect the natural frequency. There are several presumptions made for modeling and analysis when a real system is approximated to a straightforward cantilever beam.

Some conducted works have been cited here chronologically. For example, a modified theory of couple stress was applied by Akgoz and Civalek[1] to determine the natural frequencies of the tapered beam. The natural frequency of simply supported beams guided elastically at one end was investigated by Calioand Elishakoff[2].He considered the trigonometric functions of the elasticity modulus in mathematical modeling.

The static and dynamic responses of a prismatic beam were studied by Li [3], who took into account shear deformation and rotational inertia. A piecewise element was adopted by Singh and Li [4]to evaluate the performance of a cantilever column restrained by the elastic foundation and subjected to buckling load. Huang and Li [5]proposed a new method to study the free vibration of tapered beams under different conditions. The beam conditions were: clamped at two ends, simply supported, cantilever ends, and clamped-pinned, respectively. They used integral equations of Fredholm in the mathematical modeling of beams.

The stability and free vibration of a non-prismatic column were investigated by Shahba et al. [6]under boundary conditions of classical and non-classical. Shahba and Rajasekaran[7]applied the differential quadrature element method to solve the equation of motion to evaluate the tapered beam's stability under buckling and free vibration conditions. Also, the free vibration was analyzed by Kukla and Rychlewska[8]for fixed ends beams made from functionally graded materials. Again, Yilmaz et al. [9] applied the differential quadrature element approach to study the performance of non-prismatic columns under buckling conditions.

Chandran and Rajendran[10] adopted the fundamental of conversation energy to present a closed-form solution for prismatic cantilever columns under buckling conditions. Also, Shafiei et al. [11] applied the differential quadrature element method to solve the governing equations of square cross-section tapered microbeams to analyze the non-linear vibration behavior. Ranganathan et al. [12] integrated linear perturbation with the Rayleigh-Ritz methods to determine the maximum buckling load under a constant modulus of elasticity. Elishakoff et al. [13]studied column vibration and buckling by adopting the 5th-order polynomial and sharing mode. The buckling loads and natural frequencies for semi-rigid tapered beam-column were determined by Rezaiee and Masoodi[14] by closed-form solutions. Also, Lee and Lee [15] investigated the buckling and free vibration of circular and square tapered cantilever columns.

Chain et al [16] applied classical and modified Rayleigh method (CRM and MRM)with finite element (FEM) to find out the natural frequency for non-uniform cantilever beam. For beam length greater than half, good matching was achieved between CRM and FEM. From the other side, excellent matching was obtained for beam length less than half.

Du et al [17] introduced an enhanced mathematical model for free vibration analysis of rotating cantilever beam having free mass end. The model was developed based on the theory of non-linear green strain. The discrete dynamic behavior was derived by applying the Galerkin and Hamilton principle to find out the chordwise and axial motions. The model was validated with numerical calculations and the comparison revealed the dynamic response of the beam is influenced even with little end mass.

In this paper, it was presented full details of the mathematical modeling for the cantilever beam to find the Dynamic Response (the natural frequencies) under different working surrounding conditions (Temperatures). It was investigated the effect of a wide range of temperatures (-100 ℃ to 400 ℃) for the selected alloy (AISI 304 austenitic stainless steel).Thedevelopment of mathematical model was started from scratch to find the analytical solution. This analytical solution takes intoaccount the effect of the surrounding temperatures on the material properties of the beam. Consequently, it can be found the effect of the surrounding temperatures on the vibration behaviour of the cantilever beam (natural frequencies). A new Matlab code was developed to achieve the analytical solution results, considering the effect of some beam geometrical dimensions.

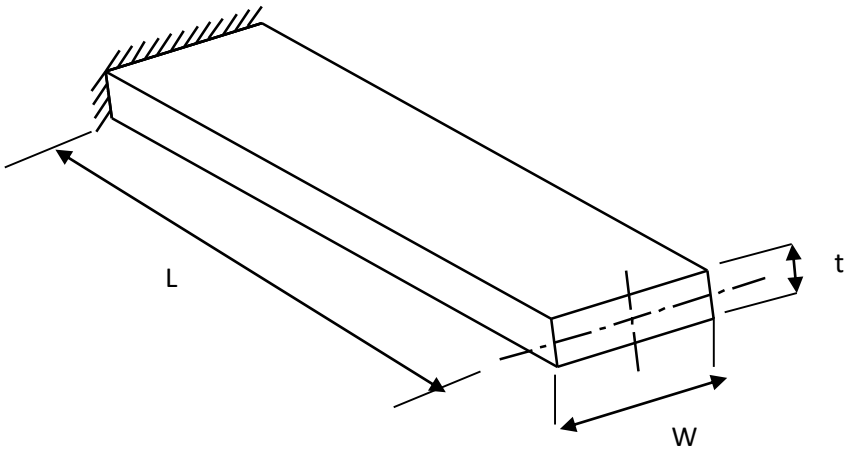

Figure 1. cantilever beam

2. Free Vibration for cantilever beam

The solution of free vibration for the cantilever beam, shown in Fig. 1, is proposed between the perpendicular and its centroidal axis.

Total Energy Relation Ships

Equation 1 shows the strain energy (V_b) of the cantilever beam under bending-bending vibration conditions [18]:

$$P_b = \int_0^l \left[\frac{EI_{yy}}{2} \left(\frac{\partial^2 q}{\partial Z^2}\right)^2 + EI_{xy} \left(\frac{\partial^2 q}{\partial Z^2}\right).\left(\frac{\partial^2 p}{\partial Z^2}\right) + \frac{EI_{xx}}{2} \left(\frac{\partial^2 p}{\partial Z^2}\right) \right] dZ \quad (1)$$

When the beam is subjected to torsional vibration, its strain Vt energy is expressed by equation 2:

$$P_t = \int_0^L \left[\frac{C}{2} \left(\frac{\partial \beta}{\partial Z}\right)^2 - \frac{E}{24} \left(\frac{\partial \beta}{\partial Z}\right).\left(\frac{\partial^3 \beta}{\partial Z^3}\right) \int_A b^2 h^3 db \right] dZ$$

(2)

Considering that the beam has a uniform cross-section with a small thickness (t). Therefore, merging the above two equations yields the c beam strain energy Punder bending-bending-torsion conditions:

$$\mathrm{P_c} = \int_0^{\mathrm{L}} \left[\frac{\mathrm{EI_{yy}}}{2} \left(\frac{\partial^2 \mathrm{q}}{\partial \mathrm{Z}^2}\right)^2 + \mathrm{EI_{xy}} \left(\frac{\partial^2 \mathrm{q}}{\partial \mathrm{Z}^2}\right).\left(\frac{\partial^2 \mathrm{p}}{\partial \mathrm{z}^2}\right) + \frac{\mathrm{EI_{xx}}}{2} \left(\frac{\partial^2 \mathrm{p}}{\partial \mathrm{z}^2}\right) + \frac{\mathrm{c}}{2} \left(\frac{\partial \beta}{\partial \mathrm{z}}\right)^2 - \frac{\mathrm{E}}{24} \left(\frac{\partial \beta}{\partial \mathrm{z}}\right).\left(\frac{\partial^3 \beta}{\partial \mathrm{z}^3}\right) \int_{\mathrm{A}} \mathrm{b}^2 h^3 \mathrm{db} \right] dZ$$

(3)

If the gravitational influence is neglected, the Pc will equal the total potential energy (P). Further, the total kinetic energy (T) of the cantilever beam exposed to integrated bending –torsion is illustrated by

$$T = \int_0^L \left[\frac{w'}{2g} \left(\frac{\partial}{\partial t} (q + r_y \beta \,) \right)^2 + \frac{w'}{2g} \left(\frac{\partial}{\partial t} (P + r_x \beta) \right)^2 + \frac{I_{c.g}}{2} \left(\frac{\partial \beta}{\partial t} \right)^2 \right] dZ$$

(4)

Thus, shown below refers to the Lagrangian function that yields from subtracting kinetic frompotential energies (L=T-P).

$$L = \int_0^L \left[\begin{array}{l} \left\{ \frac{w'}{2g} \left(\frac{\partial}{\partial t} \left(q + r_y \beta \right) \right)^2 + \frac{w'}{2g} \left(\frac{\partial}{\partial t} \left(p + r_x \beta \right) \right)^2 + \frac{I_{c.g}}{2} \left(\frac{\partial \beta}{\partial t} \right)^2 \right\} - \left\{ \frac{EI_{yy}}{2} \left(\frac{\partial^2 q}{\partial Z^2} \right)^2 \right. \\ \left. EI_{xy} \left(\frac{\partial^2 q}{\partial Z^2} \right) \left(\frac{\partial^2 p}{\partial Z^2} \right) + \frac{EI_{xx}}{2} \left(\frac{\partial^2 p}{\partial Z^2} \right)^2 + \frac{c}{2} \left(\frac{\partial \beta}{\partial Z} \right)^2 - \frac{E}{24} \left(\frac{\partial \beta}{\partial Z} \right) \left(\frac{\partial^3 \beta}{\partial Z^3} \right) \int_A b^2 h^3 \, db \right\} \end{array} \right] dZ$$

(5)

If Hamilton's principal (16) ($\int_{t0}^{t1} L dt$) is applied, we get:

$$\int_{t_o}^{t_1} L \, dt = \int_{t_o}^{t_1} \int_0^L \left[\begin{array}{l} \left\{ \frac{w'}{2g} \left(\frac{\partial}{\partial t} \left(q + r_y \beta \right) \right)^2 + \frac{w'}{2g} \left(\frac{\partial}{\partial t} \left(p + r_x \beta \right) \right)^2 + \frac{I_{c.g}}{2} \left(\frac{\partial \beta}{\partial t} \right)^2 \right\} - \left\{ \frac{EI_{yy}}{2} \left(\frac{\partial^2 q}{\partial Z^2} \right)^2 \right. \\ \left. EI_{xy} \left(\frac{\partial^2 q}{\partial Z^2} \right) \left(\frac{\partial^2 p}{\partial Z^2} \right) + \frac{EI_{xx}}{2} \left(\frac{\partial^2 p}{\partial Z^2} \right)^2 + \frac{c}{2} \left(\frac{\partial \beta}{\partial Z} \right)^2 - \frac{E}{24} \left(\frac{\partial \beta}{\partial Z} \right) \left(\frac{\partial^3 \beta}{\partial Z^3} \right) \int_A b^2 h^3 \, db \right\} \end{array} \right] dZ \, dt$$

(6)

Also, it can be expressed as in:

$$\int_{to}^{t_1} \int_0^L (\Phi) dZ \, dt$$

(7)

Where $\int_0^L (\Phi) dz = L$

Φ represents the variational function.

Equations of Motions

Fig. 1 illustrates the section of the cantilever beam with centroid to flexure center position. The principle of Hamilton [18]shows that $\int_{t_o}^{t_1} Ldt$ is applied at two fixed time points, namely, a_o and a_1 which are stationary for the dynamic trajectory. When the Euler equation is applied to the integral, the two Stationary times can be obtained as revealed in:

$$\frac{\partial \Phi}{\partial p_n} - \frac{\partial}{\partial Z}\left(\frac{\partial \Phi}{\partial p_n'}\right) - \frac{\partial}{\partial t}\left(\frac{\partial \Phi}{\partial \dot{p}}\right) + \frac{\partial^2}{\partial Z^2}\left(\frac{\partial \Phi}{\partial p_n''}\right) + \frac{\partial^2}{\partial t^2}\left(\frac{\partial \Phi}{\partial \ddot{p}_n}\right) - \frac{\partial^3}{\partial^3 Z}\left(\frac{\partial \Phi}{\partial p_n'''}\right) - \frac{\partial^3}{\partial t^3}\left(\frac{\partial \Phi}{\partial \dddot{p}_n}\right) = 0$$

(8)

Where,

$$\Phi = g\left(p_n, p_n', \dot{p}_n, p_n'', \ddot{p}_n, p_n''', \dddot{p}_n, Z, t\right)$$

(9)

Also:

$$p_n' = \frac{\partial p_n}{\partial Z} \quad , \dot{p}_n = \frac{\partial p_n}{\partial t} \quad , p_n'' = \frac{\partial^2 p_n}{\partial Z^2} \quad , \ddot{p}_n = \frac{\partial^2 p_n}{\partial t^2} \quad , p_n''' = \frac{\partial^3 p_n}{\partial Z^3} \quad , \dddot{p}_n = \frac{\partial^3 q}{\partial t^3}$$

The obtained equations are motional system equations. The integral form of equation 6 consists of three dependent parameters, namely; q, p, and β, and applying the Euler equations by replacing k_n with either q, p or β yields:

$$\left.\begin{aligned}
&\frac{\partial^2}{\partial Z^2}\left[EI_{yy}\left(\frac{\partial^2 q}{\partial Z^2}\right) + EI_{xy}\left(\frac{\partial^2 p}{\partial Z^2}\right)\right] + \frac{w'}{g}\left(\frac{\partial^2 q}{\partial t^2}\right) = -\frac{w' r_y}{g}\left(\frac{\partial^2 \beta}{\partial t^2}\right) \\
&\frac{\partial^2}{\partial Z^2}\left[EI_{xx}\left(\frac{\partial^2 p}{\partial Z^2}\right) + EI_{xy}\left(\frac{\partial^2 q}{\partial Z^2}\right)\right] + \frac{w'}{g}\left(\frac{\partial^2 p}{\partial t^2}\right) = -\frac{w' r_x}{g}\left(\frac{\partial^2 \beta}{\partial t^2}\right) \\
&B_1 \frac{\partial^4 \beta}{\partial Z^4} - B\frac{\partial^2 \beta}{\partial Z^2} + \frac{I_{c.f}}{g}\left(\frac{\partial^2 \beta}{\partial t^2}\right) = -\frac{w' r_y}{g}\left(\frac{\partial^2 q}{\partial t^2}\right) - \frac{w' r_x}{g}\left(\frac{\partial^2 p}{\partial t^2}\right)
\end{aligned}\right\} \quad \text{(10 a, b, c)}$$

Where:

$$I_{c.f} = I_{c.g} + w'.r_x^2 \quad + w'.r_y^2$$

$$B_1 = \frac{1}{12} E \int_A b^2 h^3 db$$

If the pre-twist is removed (i.e. $\lambda_t = 0$), And made Ixy equal to 0, the three parts of equation 10 are simplified to:

$$EI_{yy}\left(\frac{\partial^4 q}{\partial Z^4}\right)+\frac{w'}{g}\left(\frac{\partial^2 q}{\partial t^2}\right)=\frac{-w'}{g}r_y\left(\frac{\partial^2 \beta}{\partial t^2}\right)$$

$$EI_{xx}\left(\frac{\partial^4 p}{\partial z^4}\right)+\frac{w'}{g}\left(\frac{\partial^2 p}{\partial t^2}\right)=\frac{-w'}{g}r_x\left(\frac{\partial^2 \beta}{\partial t^2}\right)$$

$$c\left(\frac{\partial^2 \beta}{\partial z^2}\right)-I_{c.f}\left(\frac{\partial^2 \beta}{\partial t^2}\right)=\frac{w'}{g}r_y\left(\frac{\partial^2 \beta}{\partial t^2}\right)+\frac{w'}{g}r_x\left(\frac{\partial^2 p}{\partial t^2}\right)$$

(11 a, b, c)

Solution of system motion Equations

The shape functions of q, p, and β that were taken from [19] are assumed to be in the following forms:

$$Q=Sin\omega t\sum_{m=1}^{n}B_m F_m(Z)$$

$$P=Sin\omega t\sum_{m=1}^{n}A_j\left[\frac{(m+2)(m+3)}{6}\left(\frac{Z}{L}\right)^{m+1}-\frac{m(m+3)}{3}\left(\frac{Z}{L}\right)^{m+2}+\frac{m(m+1)}{6}\left(\frac{Z}{L}\right)^{m+3}\right]$$

(12a,b, c)

$$\beta=Sin\omega t\sum_{m=1}^{n}C_m\left(\frac{Z}{L}\right)^m\left(1-\left(\frac{m}{m+1}\right)\left(\frac{Z}{L}\right)\right)$$

That satisfies the following boundary conditions:

$$P=\frac{dP}{dZ}=Q=\frac{dQ}{dZ}=\beta=0 \qquad \text{when Z=0}$$

$$\frac{d^2P}{dZ^2}=\frac{d^3P}{dZ^3}=\frac{d^2Q}{dZ^2}=\frac{d^3Q}{dZ^3}=\frac{d\beta}{dZ}=0 \qquad \text{when Z=L}$$

The error in the differential equation 11a, b, c can be achieved if the proposed solution expressed by equation 12 a, b, c for u, v, and θ is used.:

$$\delta_1=\sum_r\left(EI_{yy}B_r F_r^{''''}-\left(\frac{w'}{g}\right)\omega^2 B_r F_r-\left(\frac{w'}{g}\right)r_y\omega^2 C_r F_r\right)$$

$$\delta_2=\sum_r\left(EI_{xx}A_r F_r^{''''}-\left(\frac{w'}{g}\right)\omega^2 A_r F_r+\left(\frac{w'}{g}\right)r_x\omega^2 C_r F_r\right)$$

(13 a, b, c)

$$\delta_3=\sum_r\left(C_r C F_r^{''''}+C_r F_r\left(\frac{I_{c.f}}{g}\right)\omega^2+\left(\frac{w'}{g}\right)r_y\omega^2 B_r F_r-\left(\frac{w'}{g}\right)r_x\omega^2 A_r F_r\right)$$

Three simultaneous equations can be achieved if equation 13 a, b, is subjected to the Ritz –Galerkin operation.

$$\left.\begin{aligned}&\int_0^l \delta_1 A_j F_j(Z)dZ = 0,\ j = 1,2.....n\\&\int_0^l \delta_2 B_j F_j(Z)dZ = 0,\ j = 1,2.....n\\&\text{c)}\\&\int_0^l \delta_3 C_j F_j(Z)dZ = 0,\ j = 1,2.....n\end{aligned}\right\} \quad \text{(14 a, b,}$$

The Eigenvalues are obtained when equation 14 a, b, and c is integrated to yield equation 15:

$$\begin{bmatrix}(D-E\omega^2) & (F-G\omega^2) & (H-I\omega^2)\\(J-K\omega^2) & (L-M\omega^2) & (N-O\omega^2)\\(P-Q\omega^2) & (R-S\omega^2) & (T-U\omega^2)\end{bmatrix}\begin{bmatrix}A\\B\\C\end{bmatrix}=0 \quad (15)$$

If we assume a symmetrical cross-section about principal axes (i.e., $rx = 0$ and $ry = 0$), the solution will be reduced to equation 16:

$$\begin{bmatrix}(D-E\omega^2) & (F-G\omega^2) & (H-I\omega^2)\\(J-K\omega^2) & (L-M\omega^2) & (N-O\omega^2)\\(P-Q\omega^2) & (R-S\omega^2) & (T-U\omega^2)\end{bmatrix}\begin{bmatrix}A\\B\\C\end{bmatrix}=0 \quad (16)$$

The terms *D,E,*..etc in the Eigenvalues matrix presented in equation 15 are given in equations 17-27 shown below:

$$D_{j,r} = R1\left[\frac{R2.J5}{(RJ-1)} - \frac{R2.J6+R3.J5}{RJ} + \frac{R2.J7+R3.J6+R4.J5}{(RJ+1)} - \frac{R3.J7+R4.J6}{(RJ+2)} + \frac{R4.J7}{(RJ+3)}\right] \quad (17)$$

$$E_{j,r} = \lambda_1\left[\frac{R5.J5}{(RJ+3)} - \frac{R5.J6+R6.J5}{(RJ+4)} + \frac{R5.J7+R6.J6+R7.J5}{(RJ+5)} - \frac{R6.J7+R7.J6}{(RJ+6)} + \frac{RJ.J7}{(RJ+7)}\right] \quad (18)$$

$$F_{j,r} = G_{j,r} = H_{j,r} = J_{j,r} = K_{j,r} = N_{j,r} = P_{j,r} = R_{j,r} = 0 \quad (19)$$

$$I_{j,r} = \lambda_1\ r_X\left[\frac{J5}{(RJ+2)} - \frac{J6+R8.J5}{(RJ+3)} + \frac{J7+R8.J6}{(Rj+4)} - \frac{R8.J7}{(RJ+5)}\right] \quad (20)$$

$$L_{j,r} = D_{j,r} \quad (21)$$

$$M_{j,r} = \lambda_2\left[\frac{R5.J5}{(RJ+3)} - \frac{R5.J6+R6.J5}{(RJ+4)} + \frac{R5.J7+R6.J6+R7.J5}{(RJ+5)} - \frac{R6.J7+R7.J6}{(RJ+6)} + \frac{R7.J7}{(RJ+7)}\right] \quad (22)$$

$$O_{j,r} = \lambda_2\ r_Y\left[\frac{J5}{(RJ+2)} - \frac{J6+R8.J5}{(RJ+3)} + \frac{J7+R8.J6}{(RJ+4)} - \frac{R8.J7}{(RJ+5)}\right] \quad (23)$$

$$Q_{j,r} = \lambda_3\ r_X\left[\frac{R5}{(RJ+2)} - \frac{R5.J8+R6}{(RJ+3)} + \frac{R6.J8+R7}{(RJ+4)} - \frac{R7.J8}{(RJ+5)}\right] \quad (24)$$

$$S_{j,r} = -\lambda_3 r_Y \left[\frac{R5}{(RJ+2)} - \frac{R5.J8+R6}{(RJ+3)} + \frac{R6.J8+R7}{(RJ+4)} - \frac{R7.J8}{(RJ+5)} \right] \quad (25)$$

$$T_{j,r} = \frac{R9}{(RJ-1)} - \frac{R9.J8+R10}{RJ} + \frac{R10.J8}{(RJ+1)} \quad (26)$$

$$U_{j,r} = -\lambda_3 \left(\frac{I_P}{A} + r_X^2 + r_Y^2 \right) \left[\frac{1}{(RJ+1)} - \frac{J8+R8}{(RJ+2)} + \frac{R8.J8}{(RJ+3)} \right] \quad (27)$$

Where

$$\lambda_1 = \frac{w' L^4}{E I_{XX} g}, \qquad \lambda_2 = \frac{w' L^4}{E I_{YY} g}, \qquad \lambda_3 = \frac{w' L^2}{C g}$$

$J5 = (j+2)\,(j+3)/6\,, \qquad J6 = j\,(j+3)/3\,, J7 = j\,(j+1)/6\,, J8 = j/(j+1)$

And

$R1 = r\,(r+1)\,(r+2)\,(r+3)\,, R2 = (r-1)\,(r-2)/6\,, R3 = r\,(r-1)/3\,, R4 = r\,(r+1)/6$

$R5 = (r+2)\,(r+3)/6\,, \qquad R6 = r(r+3)/3\,, \qquad R7 = r(r+1)/6\,, \qquad R8 = r/(r+1)\,,$

$R9 = r(r-1)\,, \qquad R10 = r^2\,, \qquad RJ = r + j$

It is basically that r_x^2 as well as r_y^2 are involved in the U of equation 27. Otherwise, an error will be produced in the calculated frequencies.

Developed Program

The values and parameters for the derived and integrated equations are computed by the developed computer program to calculate the natural frequencies of the cantilever beam. The developed program is given in the flow chart depicted in Fig. 2.

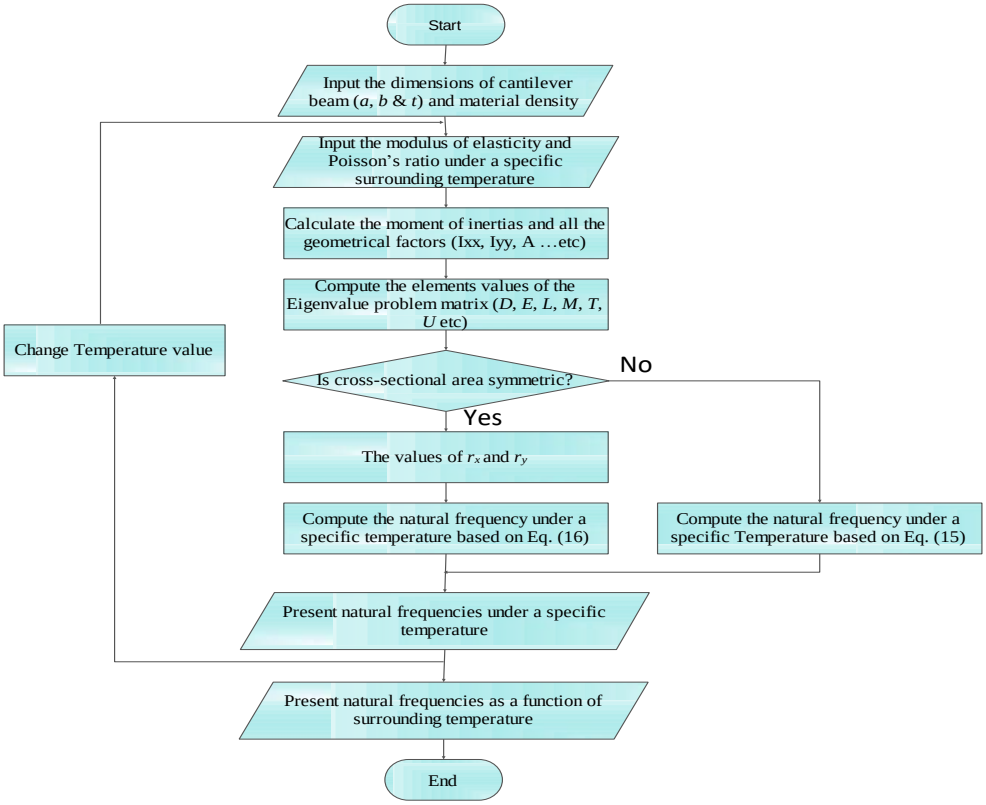

Figure 2. Flow chart of the developed Matlab code for solving the proposed analytical solution of the free vibration cantilever beam.

Verification Case

A verification case is used here to investigate the reliability of the developed analytical model [20]. The fundamental natural frequency was calculated using the proposed analytical solution over various temperatures and aspect ratios. The Young modulus of elasticity and passion ratio of the AISI 304 austenitic stainless steel for different temperatures are presented in Table 1. The density of this type of steel is $\rho = 7850 \frac{Kg}{m^3}$. The experimental results in Ref.[20]is invoked here for comparison.

Table 1. Modulus of elasticity and passion ratio of AISI 304 austenitic stainless steel for different temperatures [20]

Temperature °C	**Modulus of elasticity**	**Position ratio (v)**
-100	204	-
25	194	0.265
50	193	0.267
100	190	0.272
150	187	0.276
200	184	0.280

250	181	0.284
300	177	0.288
350	173	0.292
400	168	0.295

3. Results And Discussion

This study used different aspect ratios to involve the effect of geometry besides the temperature on the fundamental natural frequency. Also, three thicknesses of the cantilever beam are utilized: 0.001, 0.002, and 0.003 m, respectively.

Fig. 3 shows the analytical results of the principal natural frequencies at various given lengths. The experimental findings in Ref.[20] related to measuring the fundamental natural frequency for the cantilever beam at different lengths is provided here to make a fair comparison. The same different lengths used in Ref. [20]are replaced in the analytical solutions to perform a fair comparison. The figure reveals a good match between experimental and analytical solutions. The figure indicates that the fundamental natural frequency decreases with increasing beam length. If the statistical analysis for percentage errors between analytical and experimental findings is applied in terms of mean, standard deviation, max, and min, we get 0.653, ±0.093, 0.79, and 0.54, respectively.

The general trend of these figures illustrates that at any aspect ratio or thickness, the values of fundamental natural frequency decrease with increasing temperature. Also, increasing the aspect ratio, particularly at 2.5, led to a reduction in the natural frequency but less extent compared to temperature. The significant impact on the natural frequency is attributed to the beam thickness, as Fig.s 4-6 reveal. For example, the range of natural frequency (min-max) over the limits of temperature (-100-400 ℃) and aspect ratio (0.4-2.5) for the three thicknesses is found to be: (76.2956-84.6124 Hz); (152.5911-169.2247Hz); and (228.8867-253.8371 Hz) respectively. In other words, the fundamental natural frequency was strongly influenced by the beam thickness compared with temperature and aspect ratio.The effect of aspect ratio, thickness, and temperature on the fundamental natural frequency is also presented, as Fig.s 4-6 depict. The beam length for the cases in Fig.s 4-6 is taken at 0.1m, and the width is changeable to give different aspect ratios.

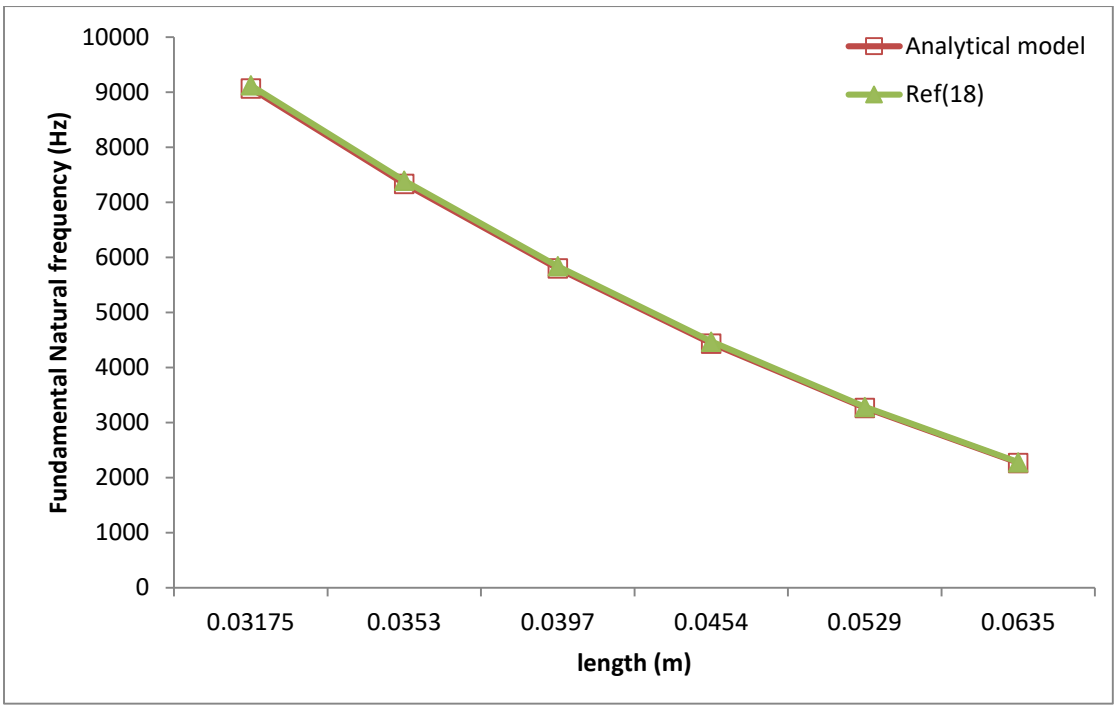

Figure3. Comparison between analytical and experimental results of the natural frequency for different beam lengths

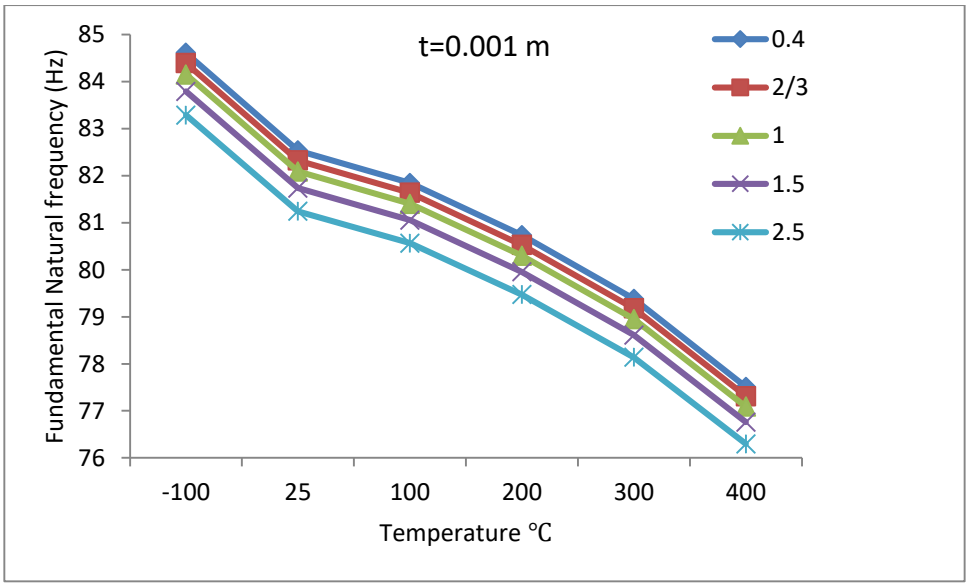

Figure 4. Effect of temperature (℃) and aspect ratio on the fundamental natural frequency (Hz) for the 0.001 m thickness beam

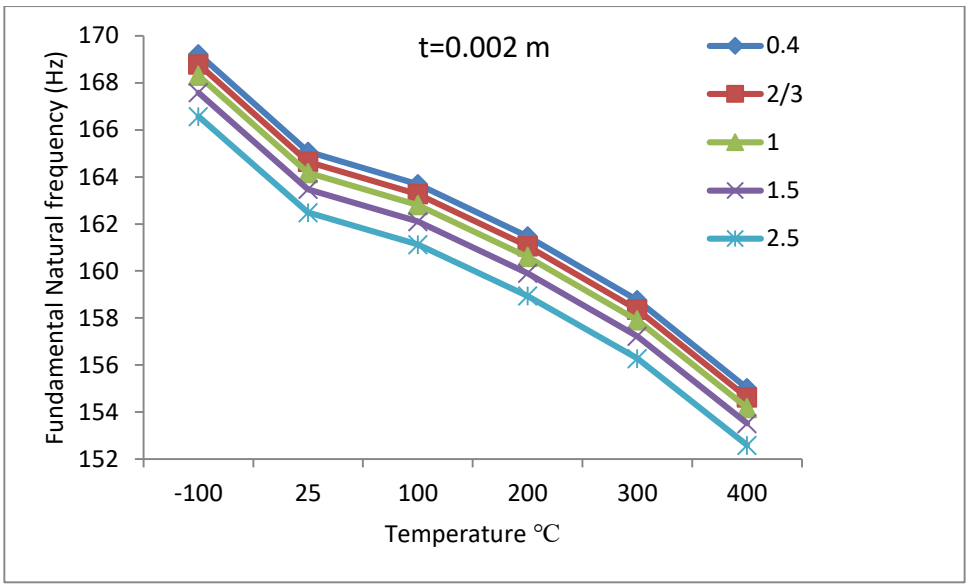

Figure 5. Effect of temperature (℃) and aspect ratio on the fundamental natural frequency (Hz) for the 0.002 m thickness beam

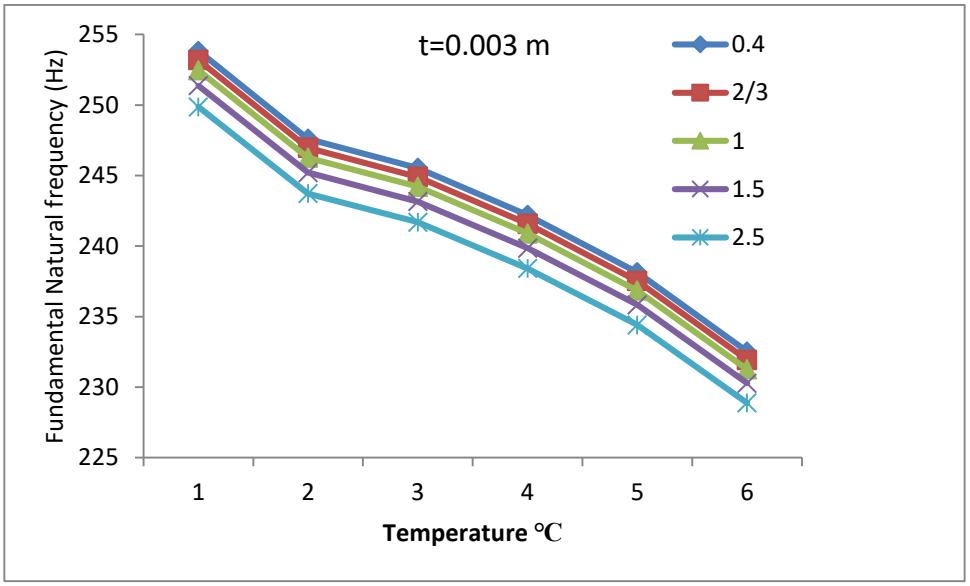

Figure 6. Effect of temperature (℃) and aspect ratio on the fundamental natural frequency (Hz) for the 0.003 m thickness beam

4. Conclusions

This study proposed an analytical solution for free vibration analysis of cantilever beam. The mathematical model was verified with experimental findings that measured fundamental natural frequency experimentally. Further, the author also studied the influence of temperature and geometrician factors represented by aspect ratio and thickness on the fundamental natural frequency. Based on the obtained findings, the following conclusions can be picked up:

1. The developed analytical solution successfully determined the fundamental natural frequency and verified it with actual experiments with a percentage error of no more than 0.79.
2. The beam thickness greatly influenced the calculated natural frequency, followed by temperature and aspect ratio.
3. The calculated natural frequency recorded high increases with increasing beam thickness while slightly decreasing with increasing temperature and aspect ratio.

References

1. Akgöz B, Civalek Ö. Free vibration analysis of axially functionally graded tapered Bernoulli–Euler microbeams based on the modified couple stress theory. *Composite Structures*. 2013 **2013**/04/01/;*98*:314-22.
2. Caliò I, Elishakoff I. Closed-form solutions for axially graded beam-columns. *Journal of Sound and Vibration.* 2005 **2005**/02/23/;*280(3):*1083-94.
3. Li XF. A unified approach for analyzing static and dynamic behaviors of functionally graded Timoshenko and Euler–Bernoulli beams. *Journal of Sound and Vibration.* 2008 **2008**/12/23/;*318(4):*1210-29.
4. Singh KV, Li G. Buckling of functionally graded and elastically restrained non-uniform columns. *Composites Part B: Engineering*. 2009 **2009**/07/01/;*40(5)*:393-403.
5. Huang Y, Li X-F. A new approach for free vibration of axially functionally graded beams with non-uniform cross-section. *Journal of Sound and Vibration*. 2010 **2010**/05/24/;*329(11):*2291-303.
6. Shahba A, Attarnejad R, Marvi MT, Hajilar S. Free vibration and stability analysis of axially functionally graded tapered Timoshenko beams with classical and non-classical boundary conditions. *Composites Part B: Engineering*. 2011 **2011**/06/01/;*42(4):*801-8.
7. Shahba A, Rajasekaran S. Free vibration and stability of tapered Euler–Bernoulli beams made of axially functionally graded materials. *Applied Mathematical Modelling*. 2012 **2012**/07/01/;*36(7):*3094-111.
8. Stanisław Kukla, Rychlewska J. FREE VIBRATION ANALYSIS OF FUNCTIONALLY GRADED BEAMS *Journal of Applied Mathematics and Computational Mechanics*. **2013**;*12(2):*39-44.
9. Yilmaz Y, Girgin Z, Evran S. Buckling Analyses of Axially Functionally Graded Nonuniform Columns with Elastic Restraint Using a Localized Differential Quadrature Method. *Mathematical Problems in Engineering.* 2013 **2013**/07/28;2013:793062.
10. GEETHU CHANDRAN, M.G.RAJENDRAN. STUDY ON BUCKLING OF COLUMN MADE OF FUNCTIONALLY GRADED MATERIAL. *International Journal of Mechanical And Production Engineering.* **2014**;*2(2):*52-4.
11. Shafiei N, Kazemi M, Ghadiri M. Nonlinear vibration of axially functionally graded tapered microbeams. *International Journal of Engineering Science*. 2016 **2016**/05/01/;*102:*12-26.
12. Ranganathan SI, Abed FH, Aldadah MG. Buckling of slender columns with functionally graded microstructures. *Mechanics of Advanced Materials and Structures*. **2016** 2016/11/01;*23(11):*1360-7.
13. Elishakoff I, Eisenberger M, Delmas A. Buckling and Vibration of Functionally Graded Material Columns Sharing Duncan's Mode Shape, and New Cases. *Structures.* 2016 **2016**/02/01/;*5*:170-4.
14. Rezaiee-Pajand M, Masoodi AR. Exact natural frequencies and buckling load of functionally graded material tapered beam-columns considering semi-rigid connections. *Journal of Vibration and Control.* **2016** 2018/05/01;24(9):1787-808.
15. Lee JK, Lee BK. Free vibration and buckling of tapered columns made of axially functionally graded materials. *Applied Mathematical Modelling.* 2019 **2019**/11/01/;75:73-87.
16. Ghani, Suadad Noori, Neamah, Raghad Azeez, Abdalzahra, Ali Talib, Al-Ansari, Luay S. and Abdulsamad, Husam Jawad. "Analytical and numerical investigation of free vibration for

stepped beam with different materials" *Open Engineering, vol. 12, no. 1,* **2022**, pp. 184-196. https://doi.org/10.1515/eng-2022-0031.

17. Du, Xiaokang, Jing Zhang, Xian Guo, Liang Li, and Dingguo Zhang. **2022**. "Dynamics Analysis of Rotating Cantilever Beams with Free End Mass" *Applied Sciences 12, no. 15*: 7553. https://doi.org/10.3390/app12157553

18. Carnegie W. Vibrations of Pre-Twisted Cantilever Blading: An Additional Effect Due to Torsion. *Proceedings of the Institution of Mechanical Engineers.* **1962** 1962/06/01;*176(1):*315-22.

19. Rao JS, Carnegie W. Solution of the equations of motion of coupled-bending bending torsion vibrations of turbine blades by the method of ritz-galerkin. *International Journal of Mechanical Sciences.* **1970** 1970/10/01/;12(10):875-82.

20. Abbas BAH, Irretier H. Experimental and theoretical investigations of the effect of root flexibility on the vibration characteristics of cantilever beams. *Journal of Sound Vibration*. 1989 May 01, **1989**;*130*:353-62.